ELSEVIER

Biochimica et Biophysica Acta 1278 (1996) 213–222

BBA Biochimica et Biophysica Acta

Saturable P-glycoprotein kinetics assayed by fluorescence studies of drug efflux from suspended human KB8-5 cells

Rick I. Ghauharali [a], Hans V. Westerhoff [b,c], Henk Dekker [a], Jan Lankelma [a,*]

[a] *Department of Medical Oncology, Free University Hospital, Room BR 232, P.O. Box 7057, 1007 MB Amsterdam, The Netherlands*
[b] *E.C. Slater Institute for Biochemical Research, BioCentrum, University of Amsterdam, Amsterdam, The Netherlands*
[c] *The Netherlands Cancer Institute, Division of Molecular Biology, Amsterdam, The Netherlands*

Received 12 May 1995; revised 11 August 1995; accepted 19 September 1995

Abstract

This article describes a new and rapid method to determine the pumping rate of P-glycoprotein (P-gp) in intact cells. Multidrug resistant (MDR) human epidermoid carcinoma KB8-5 cells (containing P-gp) were loaded with daunorubicin (DNR) in the absence or in the presence of verapamil, sufficient to inhibit DNR pumping by P-gp. In either case, the cells were resuspended in medium devoid of DNR and the subsequent increase of the DNR fluorescence intensity was measured as a function of time. For cells loaded with the same amount of drug, the free cytosolic drug concentration ($C_i(t)$) was a unique function of the DNR medium concentration ($C_o(t)$). The cellular drug content in the presence of verapamil decreased nonlinearly with decreasing extracellular drug concentration, indicating that the intracellular drug apparent distribution volume increased with decreasing cellular drug content. At each fluorescence intensity, we calculated the P-gp mediated (verapamil-inhibitable) DNR transport rate from the rate of increase of the DNR fluorescence intensity in the absence of verapamil minus the rate of increase of the DNR fluorescence intensity in the presence of verapamil. When plotted against the intracellular free drug concentration (as calculated from the total cellular drug content and a separately determined relation between the total cellular drug content and the intracellular free drug concentration: the apparent distribution volume), this P-gp mediated DNR transport rate showed saturation of P-gp at higher DNR concentrations. The results imply that P-gp mediated DNR transport is saturable (the value of K_M is in the order of 1 μM).

Keywords: Multidrug resistance; P-glycoprotein; Glycoprotein; Pump kinetics; Fluorescence quenching; Daunorubicin

1. Introduction

P-glycoprotein (P-gp) can protect cells against lipophilic toxic compounds, among which are cytotoxic drugs [1–4]. Strong evidence has been obtained for an active transport process for these compounds across the plasma membrane of P-gp containing cells [5,6]. Total cellular drug uptake is affected by additional processes, such as passive drug leak across the plasma membrane [7,8], uptake by cellular organelles [9–12] and binding to macromolecules [13]. To understand the effect of P-gp on drug resistance and its reversal by modifiers, such as verapamil [14], the dependence of drug uptake on the kinetic and thermodynamic properties of all these processes should be dissected.

One important determinant of drug uptake into multidrug resistant (MDR) cells is P-gp itself. A number of studies have zoomed in on the kinetics of drug pumping by this protein [8,15–18]. Of these, the studies in which P-gp functions in intact cells are of great interest. Such studies however, have to deal with the complication that the intracellular free drug concentration cannot be assessed nor controlled directly. Spoelstra et al. [8] estimated the intracellular free daunorubicin (DNR) concentration from the passive leak rate and a predetermined passive permeation coefficient. The variation of the P-gp pump rate, as measured in a flow-through system at various concentrations of extracellular DNR, combined with the calculated intracellular free drug concentration, suggested that P-gp has saturable kinetics in terms of the estimated intracellular free DNR concentrations.

Substrate saturability has the implication that at high substrate concentrations, the pump should function comparatively ineffectively. Also the half-life of drug efflux

Abbreviations: MDR, multidrug-resistant/resistance; P-gp, P-glycoprotein; DNR, daunorubicin; Hepes, *N*-(2-hydroxyethyl)piperazine-*N'*-2-ethane sulfonic acid.

* Corresponding author. Fax: +31 20 4443844.

0005-2736/96/$15.00 © 1996 Elsevier Science B.V. All rights reserved
SSDI 0005-2736(95)00224-3

into drug free medium should decrease with time. It is this latter implication that is tested in this paper and then used to assess the kinetic properties of the drug efflux pump in a new manner. Drug efflux is followed in time in a spectrofluorometer. We show how both the pumping rate and the intracellular substrate concentration are calculated by computerized fluorometry and data processing.

2. Materials and methods

2.1. Cell culture

The human epidermoid carcinoma cell line KB8-5 [19], selected by exposure to increasing concentrations of colchicine, was obtained from the American Type Culture Collection (Rockville, MD, USA). Cells were grown in monolayer in Nunc flasks (Roskilde, Denmark) in (bicarbonate-buffered) Dulbecco's modified Eagle's medium (Flow Laboratories, Irvine, UK), supplemented with 20 mM Hepes (Serva, Heidelberg, Germany) and 10% heat-inactivated fetal calf serum (FCS) (Gibco, Paisley, UK) under an atmosphere containing 5–6% CO_2 at 37°C. The cells were cultured with a selecting drug (25 nM colchicine) as described [19] until 2 to 7 days before experiments and were free of Mycoplasma, as tested with the Mycoplasma T.C. kit (Genprobe, San Diego, CA, USA). The DNR concentration needed to kill 50% of the cells was 50 nM at continuous presence in the medium for three to four days. At the conditions used for the efflux experiments in this paper, the viability as measured with Trypan blue was $> 95\%$.

2.2. Drug efflux measurements

For DNR efflux measurements, exponentially growing cells were trypsinized and kept in suspension in a growth medium referred to as medium A, supplemented with 5% FCS. Medium A is based on phosphate buffered saline (PBS) Dulbecco's formula (modified) (Flow Laboratories) to which amino acids for minimum essential medium Eagle (modified) (Flow Laboratories), Hepes (20 mM), glucose (1 g l^{-1}, Baker, Deventer, The Netherlands) and L-glutamine (4 mM, ICN Biochemicals, Cleveland, OH, USA) are added. The pH is adjusted to 7.4.

Cells were loaded in this medium with DNR for 30 min at 37°C in the absence and in the presence of 50 μM verapamil to inhibit DNR efflux by P-gp (in accordance with common practice, the rate of drug export is called 'drug efflux'). In one set of experiments, the DNR concentrations in the absence and presence of verapamil were 15 μM and 3 μM, respectively. In another set of experiments these concentrations were 25 μM and 15 μM. These specific concentrations were chosen to result in loading with the same amount of DNR in the plus and minus verapamil case. After two washing steps with DNR free medium (at room temperature) either $1 \cdot 10^5$ or $2 \cdot 10^5$ cells (as determined with a hemocytometer) were suspended in 200 μl of DNR-free medium. This suspension was then transferred to a quartz cuvette (QS, 10.00 mm path length) containing 2.5 ml of DNR-free medium at 37°C. In the minus verapamil experiments, both the washing medium and the efflux medium were verapamil free. In the plus verapamil experiments, these media were supplemented with 50 μM verapamil.

During incubation, DNR is intercalated in DNA, leading to a quenching of the DNR fluorescence intensity. During drug efflux, DNR is released from DNA, leading to an increase in the DNR fluorescence intensity, relative to the start of efflux. This increase of the DNR fluorescence intensity was monitored using a spectrofluorometer (SPEX Industries Inc., Model FluoroMax™, Edison, NJ, USA) equipped with a Xenon lamp and a thermostatted cuvette-chamber. Excitation was at 480 nm, emission was detected at 590 nm, through a 1 mm slit for both excitation and emission. The cell suspension was stirred continuously using a cell spinbar® (Bel-Art Products, Pequannock, NJ, USA) and the temperature of the cuvette was kept at 37°C. During both incubation with DNR, washing and DNR efflux, methylamine (10 mM) was present in the medium to decrease the effects of DNR entrapped in acidic intracellular compartments. At the end of the experiment digitonin was added for plasma membrane permeabilization (total concentration 30 μM).

The relationship between total cellular drug content and intracellular free drug concentration, the apparent distribution volume, was determined by exposing cells at low cell density and at high verapamil concentration to various drug concentrations for at least 30 min and measuring (after washing) how much (radiolabelled) drug had accumulated in the cells (Q_i below).

2.3. Chemicals

Daunorubicin hydrochloride was obtained from Specia (Paris, France). Verapamil, methylamine and digitonin (50% pure) were from Sigma (St. Louis, MO, USA).

2.4. Data processing

2.4.1. Mathematical analysis

For the analysis of DNR transport across the plasma membrane, we assume a three compartment model. Two compartments are the extracellular medium and a cellular space (e.g., cytosol) with equal fluorescence quantum yields for DNR. It is assumed that P-gp pumps between these compartments. The third compartment is assumed to equilibrate with the second compartment in terms of the DNR activity but quenches the DNR fluorescence intensity. This assumption was valid because the time constant of drug

release from the fluorescence intensity quenching sites was smaller than the time constant of drug release into the extracellular medium (see also the Results section). The most likely cause for quenching of cellular DNR is intercalation in nuclear DNA [13,20,21]. The third compartment is mostly nuclear DNA. DNR transport across the plasma membrane will be described as the sum of a passive component (diffusion) and an active component (P-gp mediated transport).

In appendix A we show how to calculate the free drug concentration difference across the plasma membrane as a function of time and the active (P-gp mediated) transport rate as a function of the free drug concentration difference across the plasma membrane from experimental data. Then the intracellular free drug concentration as a function of time is calculated from the total cellular DNR content (which is calculated from experimental data) and an experimentally determined relation between in the total cellular DNR content and the intracellular free drug concentration. Combination of these results yields the active transport rate as a function of the intracellular free drug concentration. In this section, we summarize the results and refer to appendix A for a detailed analysis.

The free drug concentration difference across the plasma membrane can be written as:

$$C_i(t) - C_o(t) = \frac{F_{eq} - F_{\pm Vp}(t)}{1 - q_{\pm Vp}} \cdot \frac{\varepsilon V_{tot}(C_i(t))}{V_{out} V_{cells}(C_i(t))} + \frac{\varepsilon F_1}{V_{out}} \left(\frac{V_{cells}(C_{i,eq})}{V_{cells}(C_i(t))} \cdot \frac{V_{tot}(C_i(t))}{V_{tot}(C_{i,eq})} - 1 \right) \quad (1)$$

in which $C_i(t)$ (mol l^{-1}) and $C_o(t)$ (mol l^{-1}) are the intracellular and extracellular free DNR concentrations, respectively. $F_{\pm Vp}(t)$ (counts per s, cps) is the detected DNR fluorescence intensity as a function of time in the absence or presence of verapamil (representing both the medium fluorescence intensity and the cellular DNR fluorescence intensity), F_{eq} (cps) is the DNR fluorescence intensity after membrane permeabilization and equilibration of DNR across the plasma membrane and $q_{\pm Vp}$ is the so-called quenching factor, defined as the ratio of the cellular DNR fluorescence intensity at the start of efflux (referred to as $F_{\pm Vp}(t = 0)$ (cps)) and the DNR fluorescence intensity that would be obtained if all the DNR were free in the extracellular solution after efflux and no cellular DNR quenching would occur (referred to as F_1 (cps)). V_{out} (l) and $V_{cells}(C_i(t))$ (l) represent the extracellular and the apparent distribution volume for DNR of the cells, respectively. The apparent total volume, $V_{tot}(C_i(C))$ (l), is defined as the sum of the former and ε (mol cps^{-1}) is a constant relating the medium DNR fluorescence intensity to the amount of DNR in the medium.

The active DNR transport rate, J_p (mol s^{-1} $(10^6$ cells$)^{-1}$), can be written as:

$$J_p = J_{-Vp} - J_{+Vp} \quad (2)$$

in which $J_{\pm Vp}$ (mol s^{-1} $(10^6$ cells$)^{-1}$) represents the transport rate in the absence or presence of verapamil, which is related to the measured DNR fluorescence intensity through:

$$J_{\pm Vp}(C_i(t), C_o(t)) = \frac{\varepsilon}{1 - q_{\pm Vp}} \frac{d}{dt}\left(F_{\pm Vp}(t)\right) \quad (3)$$

Eqs. (1), (2) and (3) yield J_p as a function of the free drug concentration difference across the plasma membrane.

The variation of the amount of intracellular drug with time can be obtained from:

$$Q_i(t) \approx \varepsilon \frac{F_{eq} - F_{+Vp}(t)}{1 - q_{+Vp}} \quad (4a)$$

The intracellular free drug concentration at time t is related to the total cellular drug content, $Q_i(t)$. To the extent that the binding constant of the drug to DNA varies with the intracellular drug concentration, $V_{cells}(C_i)$ varies with C_i. We assume that the dependence of $V_{cells}(C_i)$ on C_i is the same for the experiments in the presence and absence of verapamil. $V_{cells}(C_i)$ was measured by titrating with DNR and measuring the cellular DNR accumulation in the presence of verapamil (at which the pumping of DNR was inhibited) and at equilibrium (when the intracellular free drug concentration equalled the extracellular free drug concentration).

$$V_{cells}(C_i) = \frac{Q_i}{C_{i,+Vp}} \quad (4b)$$

and

$$C_i(t) = \frac{Q_i(t)}{V_{cells}(C_i)} \quad (4c)$$

2.5. Numerical analysis

The efflux curves were numerically processed in pairs (plus-and minus-verapamil) in seven steps. Discriminating between $F_{\pm Vp}(t)$ curves (fluorescence intensity as a function of (efflux) time) and $\dot{F}(\Delta F)_{\pm Vp}$ curves (rate of increase of the fluorescence intensity as a function of the fluorescence intensity difference $F_{eq} - F_{\pm Vp}(t)$) the procedure was as follows:

2.5.1. $F_{\pm Vp}(t)$ based calculations:

(1) Calculation of the curve $F_{eq} - F_{\pm Vp}(t)$ as a function of time, followed by noise reduction with a nine-point moving average filter

(2) Data compression by discarding eight of every nine points in the filtered data set

(3) Calculation of the difference quotient, representing the drug efflux rate

$$\frac{\Delta\left(F_{eq} - F_{\pm Vp}(t)\right)}{\Delta t} = \frac{\left(F_{eq} - F_{\pm Vp}(t_{i+1})\right) - \left(F_{eq} - F_{\pm Vp}(t_i)\right)}{t_{i+1} - t_i} = -\frac{\left(F_{\pm Vp}(t_{i+1}) - F_{\pm Vp}(t_i)\right)}{t_{i+1} - t_i} \quad (5)$$

as a function of $(F_{eq} - F_{\pm Vp}(t))/(1 - q_{\pm Vp})$

2.5.2. $\dot{F}(\Delta F)_{\pm Vp}$ based calculations:

(4) Interpolation of the plus-verapamil curve with a fifth order polynomial and calculation of the drug efflux rate of the plus-verapamil curve at $(F_{eq} - F_{-Vp}(t))/(1 - q_{-Vp})$ values of the minus-verapamil curve

(5) Calculation of the difference curve: drug efflux rate in the minus-verapamil case minus drug efflux rate in the plus-verapamil case at equal magnitude of $(F_{eq} - F_{-Vp}(t))/(1 - q_{-Vp})$

(6) Calibration of the y-axis using:

$$\frac{d\left(F_{eq} - F(t)_{\pm Vp}\right)}{dt} = -\frac{d\left(F_{\pm Vp}(t)\right)}{dt} = -\frac{(1 - q_{\pm Vp})}{\varepsilon}\frac{d(Q_o(t))}{dt} = \frac{(1 - q_{\pm Vp})}{\varepsilon}\frac{d(Q_i(t))}{dt} \quad (6)$$

7. Calibration of the x-axis of the difference curve using Eq. (4).

3. Results

3.1. The fluorescence signal during DNR efflux

Fig. 1 represents the increase of the DNR fluorescence intensity during efflux from KB8-5 cells in the presence (dotted line) and in the absence (solid line) of verapamil in a representative experiment. The first 64 s represent the baseline: the emission intensity of cuvette and drug free efflux medium. At $t = 64$ s the incubated cell suspension is transferred to the cuvette. The immediate increase in the fluorescence intensity represents the sum of cellular autofluorescence and scattering (minor contribution) and cellular DNR fluorescence (major contribution). As DNR was released from DNA during efflux, a gradual increase of the DNR fluorescence intensity was observed. At the end of the experiment, digitonin was added for plasma membrane permeabilization. From the subsequent rapid rise of the fluorescence intensity, it was concluded that equilibration with intracellular binding was relatively quick. Addition of digitonin in earlier phases of the experiment also showed a relatively rapid increase of the signal (data not shown), indicating that also in phases of more rapid change, the plasma membrane permeability controlled DNR efflux. For the plus-verapamil case, the addition of digitonin hardly affected the fluorescence intensity after efflux of DNR, confirming that $V_{cells}(C_i(t))/V_{tot}(C_i(t))$ was negligible.

3.2. Determination of the cellular quenching factor $q_{\pm Vp}$

Titration with DNA of a solution containing 1 μM DNR resulted in a quenching of the DNR fluorescence intensity, down to 5% of the initial value, in agreement

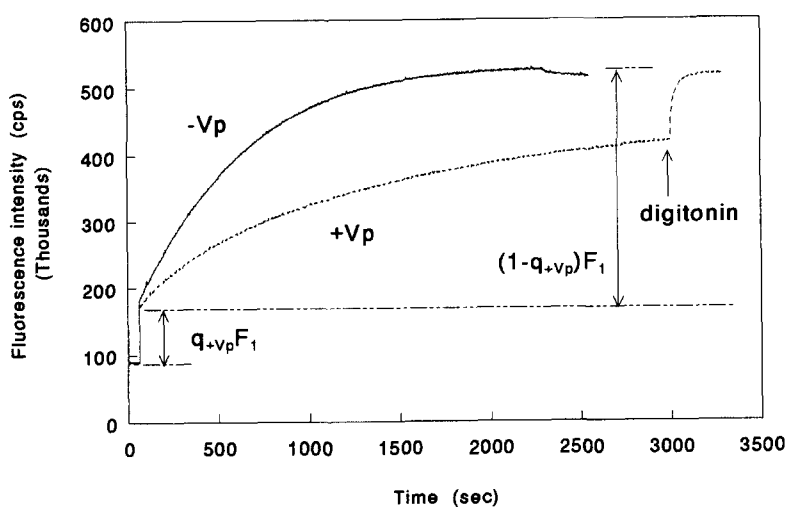

Fig. 1. Fluorescence signal (excitation and emission wavelengths 480 and 590 nm, respectively) of daunorubicin during efflux from human multidrug resistant KB8-5 cells in the absence (solid line) and in the presence (dashed line) of 50 μM verapamil. Before efflux, the cells were loaded for 30 min at 37°C in presence and in absence of verapamil with 15 μM and 25 μM daunorubicin, respectively. At the end of the experiment, digitonin was added for plasma membrane permeabilization (total concentration 30 μM). The cell density was $3.7 \cdot 10^4$ cells ml^{-1}.

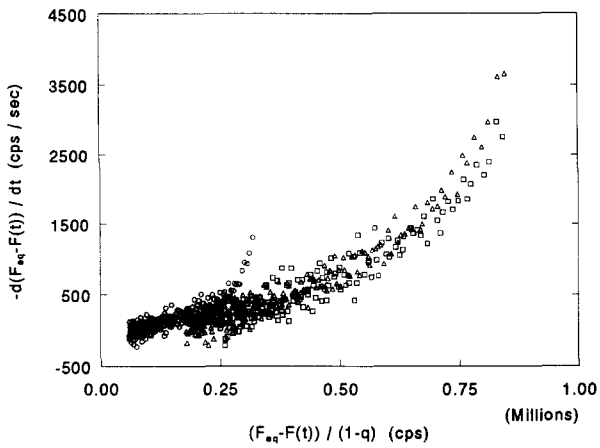

Fig. 2. The slopes of three plus-verapamil curves representing the drug efflux rate of three different experiments plotted against the normalized $(F_{eq} - F_{+Vp}(t))/(1 - q_{+Vp})$ using $q_{+Vp} = 0.19$. Experimental parameters: DNR incubation concentration: 15 μM, cell density: $3.7 \cdot 10^4$ cells ml^{-1} (squares), DNR incubation concentration: 15 μM, cell density: $7.4 \cdot 10^4$ cells ml^{-1} (triangles), DNR incubation concentration: 3 μM, cell density: $7.4 \cdot 10^4$ cells ml^{-1} (circles). Both the y-axis and the x-axis were normalized with respect to differences in cell density (see text for additional details). The y-axis shows the passive efflux rate as calculated from the primary data (unit: counts per second (cps) per second).

with a previous report [13]. The cellular quenching factor in the minus verapamil case, q_{-Vp}, was determined from the ratio of the initial fluorescence intensity and the final fluorescence intensity in the minus-verapamil efflux curve. Assuming that the DNR fluorescence intensity just before addition of digitonin in the minus-verapamil case, $F_{-dig,-Vp}(t \rightarrow \infty)$, represents F_1, q_{-Vp} was estimated as

$$q_{-Vp} = \frac{F_{-Vp}(t=0)}{F_{-dig,-Vp}(t \rightarrow \infty)} = 0.24$$

Under the assumption that in both the minus- and plus-verapamil case, the cells were loaded with the same *amount* of drug, $F_{-dig,-Vp}(t \rightarrow \infty)$ also represents F_1 in the plus-verapamil case:

$$q_{+Vp} = \frac{F_{+Vp}(t=0)}{F_{-dig,-Vp}(t \rightarrow \infty)} = 0.19$$

These results are consistent with values reported previously [22].

3.3. Drug efflux rates

As described by Eq. (3), the rate at which the DNR fluorescence intensity increases should be proportional to the DNR efflux rate. We began by analyzing the kinetics of the passive (i.e., the verapamil insensitive) DNR flux. Fig. 2 shows the slopes of plus-verapamil curves of three different experiments, plotted against the normalized $(F_{eq} - F_{+Vp}(t))/(1 - q_{+Vp})$. We refer to the axes as 'normalized axis' after correction for differences in cell density: both the y-axis and the x-axis depend on the cell density, the y-axes since the measured efflux rate depends on the number of cells present and the x-axis since the apparent distribution volume depends on the number of cells present.

Each curve shows a deviation from linearity (i.e., towards higher slopes) at higher values of the normalized $(F_{eq} - F_{+Vp}(t))/(1 - q_{+Vp})$ (or at the start of DNR efflux) when compared to the other curves at the same normalized $(F_{eq} - F_{+Vp}(t))/(1 - q_{+Vp})$. Part of this deviation may be due to a change of the apparent distribution volume with the intracellular free drug concentration. An increase of the apparent distribution volume may arise when during DNR efflux, the cellular binding sites change from a saturated to a non-saturated state. This increase of the apparent distribution volume during the first phase of DNR efflux may have led to the rapid decrease of the rate of change of the intracellular free DNR concentration during this phase. We have indications that saturation of cellular binding sites occurs at approx. 10 μM free cytosolic DNR concentration. Therefore, this effect may be expected in the high-incubation concentration experiments (triangles and squares) but not in the low-incubation concentration experiments (circles). The effect of a change of the apparent distribution volume during the first phase of efflux is taken into account in the mathematical analysis in Eq. (4). We hypothesized that the remaining part of the deviation was due to a small percentage of damaged cells (in which the plasma membrane cannot control drug efflux anymore) or due to interference of a de-quenching signal from DNR multimers attached to the plasma membrane with a high fluorescence quenching [22]: in another study

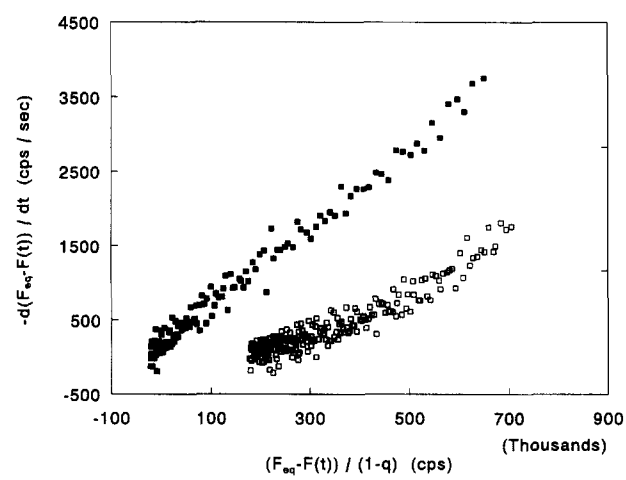

Fig. 3. The slopes of the plus-verapamil (open squares) and minus-verapamil (closed squares) curves representing the drug efflux rate plotted against the normalized $(F_{eq} - F_{\pm Vp}(t))/(1 - q_{\pm Vp})$ using $q_{+Vp} = 0.19$ and $q_{-Vp} = 0.24$ for a representative experiment. Experimental parameters: plus-verapamil DNR incubation concentration: 15 μM, minus-verapamil DNR incubation concentration: 25 μM, cell density: $3.7 \cdot 10^4$ cells ml^{-1}. The y-axis shows the drug efflux rate as calculated from the primary data (unit: cps per second) expressed per $1 \cdot 10^6$ cells. The normalization of the x-axis of Fig. 2 was used for the x-axis of this figure (see text for additional details).

[23], we found more evidence for adsorbed DNR by fluorescence resonance energy transfer measurements, using a fluorescent plasma membrane probe. Within this hypothesis, the effect of the disturbance on the initial DNR fluorescence intensity is minimal, but it can produce errors in the estimate of F_1, the DNR fluorescence intensity if all *intra*cellular DNR were free in solution. This could potentially lead to a systematic error in $q_{\pm Vp}$. However, since the calculated values for q_{-Vp} and q_{+Vp} are in the same range as reported previously [22], the error in F_1 is likely to be small. Since, within this hypothesis, this remaining part of the deviation is not specifically related to the drug efflux process, we deleted this part from the data set. From the non-overlapping part of the curve representing the experiment carried out at the low-incubation concentration (circles), we estimate that at 60 s after the start of drug efflux, most of the remaining part of the deviation does not contribute to the relevant signal anymore. We therefore deleted this part of each data set and used the remaining data for further calculations.

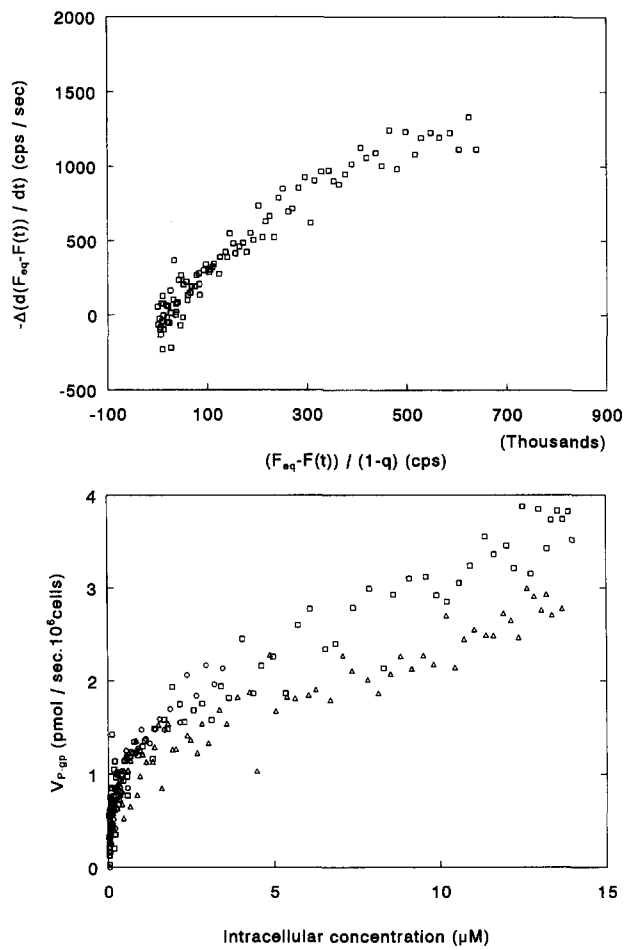

Fig. 4. (a, top) The slope of the minus-verapamil curve minus the slope of the plus-verapamil curve ($-\Delta(\mathrm{d}(F_{eq}-F_{\pm Vp}(t))/\mathrm{d}t)$) plotted against the normalized $(F_{eq}-F_{+Vp}(t))/(1-q_{+Vp})$ (which is related to the intracellular free drug concentration (see text for details)) for a representative experiment. Experimental parameters: plus-verapamil DNR incubation concentration: 15 μM, minus-verapamil DNR incubation concentration: 25 μM, cell density: $3.7\cdot10^4$ cells ml^{-1}. Both the y-axis and the x-axis were normalized to $1\cdot10^6$ cells. (b, bottom) P-gp mediated DNR efflux rate, $V_{P\text{-}gp}$, plotted against the intracellular free DNR concentration, C_i, for three different experiments. Experimental parameters: plus-verapamil DNR incubation concentration: 15 μM, minus-verapamil DNR incubation concentration: 25 μM, cell density: $3.7\cdot10^4$ cells ml^{-1} (squares), plus-verapamil DNR incubation concentration: 15 μM, minus-verapamil DNR incubation concentration: 25 μM, cell density: $7.4\cdot10^4$ cells ml^{-1} (triangles), plus-verapamil DNR incubation concentration: 3 μM, minus-verapamil DNR incubation concentration: 10 μM, cell density: $7.4\cdot10^4$ cells ml^{-1} (circles). The y-axis was calibrated using Eq. (6), the x-axis using Eq. (4). The common part of the three curves suggests a certain invariance towards the varied experimental parameters. The deviation towards lower pump rates at higher intracellular DNR concentrations indicates saturation of P-gp.

In Fig. 3 the slopes of the plus- and minus-verapamil curves (as shown in Fig. 1) of a representative experiment are plotted against the normalized $(F_{eq}-F_{\pm Vp}(t))/(1-q_{\pm Vp})$. Since each curve contains values of the slope at slightly *different* values of the normalized $(F_{eq}-F_{\pm Vp}(t))/(1-q_{\pm Vp})$, the difference curve (slope of the minus-verapamil curve minus slope of the plus-verapamil curve as a function of the normalized $(F_{eq}-F_{-Vp}(t))/(1-q_{-Vp})$) cannot be calculated directly. Therefore, the plus-verapamil curve was interpolated with a fifth order polynomial and this polynomial was used to calculate the slope of the plus-verapamil curve at the normalized $(F_{eq}-F_{-Vp}(t))/(1-q_{-Vp})$ values of the minus-verapamil curve.

According to Eq. (1), $(F_{eq}-F_{-Vp}(t))/(1-q_{-Vp})$ is related to the free drug concentration difference across the plasma membrane, $C_i(t)-C_o(t)$. In Fig. 4a the resulting difference curve of Fig. 3 is plotted. It shows that the pump rate is a saturable function of the intracellular free drug concentration.

In Fig. 4b we calibrated and refined the results plotted in Fig. 4a with Eq. (4) for the three experiments described. The results of this calculation show a common part, which suggests an invariance (to some extent) towards certain experimental parameters. The deviation towards lower pump rates at higher intracellular DNR concentrations indicates saturation of the active pump.

If the active component of DNR transport is described by a Michaelis-Menten type process, it follows from Fig. 4b that the free cytosolic DNR concentration at $V_{max}/2$ is 1 μM and V_{max} is 3 pmol s^{-1} (10^6 cells)$^{-1}$. The experiment carried out at the lower incubation concentrations did not show saturation to the same extent as the experiments performed at the higher incubation concentrations. This suggests that at this incubation concentration, in this cell line, complete saturation of P-gp has not occurred yet.

4. Discussion

In this article we described a method to determine K_M and V_{max} values for P-gp mediated DNR transport in a dynamic way, making use of the change of the DNR fluorescence intensity during DNR efflux from intact cells.

The method is based on the following principles. The internal substrate is divided between a bound and a free form, which are in rapid equilibrium. The measured fluorescence intensity is proportional to the total free substrate, both inside and outside the cell, the bound form being quenched. Because of the rapid equilibration of DNA binding, intracellular DNR behaves as a single pool, subject to intermediate fluorescence intensity quenching. The rate of change of the fluorescence intensity during drug efflux should reveal the rate of drug export at various intracellular drug concentrations and should allow one to relate the pumping rate to the drug concentration. In essence, we measured the quenching factor and derived for each time point the drug export rate from the rate of change of the fluorescence intensity. Using a calibration curve determined under equilibrium conditions, we calculated the intracellular free drug concentration (thermodynamic activity) at each time point from the amount of drug that is still in the cells. We then related the time varying export rate to the time varying intracellular free drug concentration.

Because drug pumping is active transport and because the extracellular volume is much larger than the intracellular volume (so the extracellular drug concentration remains low), the extracellular drug will not influence the pumping rate.

The kinetic parameters obtained are similar to values reported previously, using a flow-through system [8]. In that study, the passive influx was measured after a rapid inhibition of P-gp mediated DNR efflux in steady state (and leaving the intracellular drug concentration intact for a while). The method presented in this article does not require the specialized set-up of a flow-through system, but uses only fluorometry. This method may be applied to rapidly screen toxic compounds for kinetic properties of drug resistance.

For simplicity, this paper has been formulated in the sense that P-gp pumps from the cytosol. It has been suggested that P-gp pumps directly from the membrane, preventing any drug from entering the cytosol [2,24]. In the cells used in this paper, drug fluorescence was observed in the cytoplasm and in the nucleus by fluorescence microscopy. The fluorescence intensity quenching of the drug is due to its binding to DNA (fluorescence intensity quenching upon addition of digitonin is DNase I sensitive; data not shown). Virtually all of the drug effluxing from the cells in the experiments presented in this paper, ultimately derives from the drug bound to intracellular DNA. Most likely, therefore, the effluxing drug has gone through the cytosol. Our results do not specify whether or not the active extrusion of the drug from the cell is due to pumping from the cytosol or pumping from the membrane. However, if pumping was from the membrane, the membrane concentration of the drug should respond effectively to changes in the cytosol and DNA. The drug pump in our KB8-5 cells cannot be a 100% effective vacuum cleaner. Independent of the mechanism, our results demonstrate that drug pumping exhibits saturable kinetics in terms of the concentration of the bulk of intracellular drug.

The K_M for P-gp mediated DNR transport lies predominantly above drug plasma concentrations [25]. Therefore the relative contribution of a given amount of P-gp to the total drug transport rate (i.e., the ratio of the active pump rate and the total (passive and active) efflux rate) is large, when compared to a situation in which the drug plasma concentrations would lie above the K_M at a given pumping rate. This implies that toxic compounds or metabolites for which the drug plasma concentrations are above the K_M (at the same V_{max}/K_M, such that at much lower substrate concentrations the pumping rate is the same at equal substrate concentrations), may be preferable anticancer drugs in cases in which P-gp plays an important role in drug resistance.

Acknowledgements

The authors thank Sipko Mülder for helpful discussions and Lloyd Ghauharali for careful reading of the manuscript.

Appendix A

The objective of this theoretical description of DNR transport across the plasma membrane is to calculate the rate of P-gp mediated transport as a function of the intracellular free drug concentration. The analysis is divided in four parts. In the first part, the kinetic model is defined and the assumptions are outlined. In the second part, the free drug concentration difference across the plasma membrane as a function of time is calculated from experimental data. In the third part, the rate of P-gp mediated transport is calculated as a function of the free drug concentration difference across the plasma membrane from experimental data and the results from the second part. In the fourth part, the intracellular free drug concentration is calculated from the total cellular DNR content (which is calculated from experimental data) and an experimentally determined relation between the total cellular drug content and the intracellular free drug concentration: the apparent distribution volume. Combination of these results yields the rate of P-gp mediated transport as a function of the free intracellular drug concentration.

A.1. Kinetic model and assumptions

DNR transport across the plasma membrane will be described with a three compartment model: the extracellular space, a cellular space (e.g. cytosol) and a compartment which equilibrates rapidly with the cellular space, but quenches the DNR fluorescence intensity. Drug transport is described as the sum of a passive component (diffusion)

and active component (P-gp mediated). P-gp is assumed to pump between the extracellular and the cellular space.

The rate of passive free drug transport across the membrane (referred to as the leak rate), $J_l(C_i(t), C_o(t))$ (mol s^{-1} $(10^6$ cells$)^{-1}$), will in general dependent on both the intracellular and extracellular free drug concentration:

$$J_l(C_i(t),C_o(t)) = f_l(C_i(t),C_o(t)) \quad \text{(A1)}$$

in which $C_i(t)$ (mol l^{-1}) and $C_o(t)$ (mol l^{-1}) represent the intracellular and extracellular free drug concentration, respectively and the form of $f_l(C_i(t),C_o(t))$ describes the explicit dependence. The active component of free drug transport is assumed to be independent of the extracellular drug concentration. The rate of active transport (referred to as the pump rate), $J_p(C_i(t))$ (mol s^{-1} $(10^6$ cells$)^{-1}$), can be written as:

$$J_p(C_i(t)) = f_2(C_i(t)) \quad \text{(A2)}$$

in which the form of the function $f_2(C_i(t))$ depends on the specific model used to describe DNR transport across the plasma membrane. In the main text, the data are analyzed in the context of a Michaelis-Menten model.

Most likely the main depot of intracellular quenched DNR is cellular DNA. Because of the rapid equilibrium between intracellular free DNR and DNA bound DNR, we will consider a single pool of cellular DNR with intermediate quenching.

A.2. Calculation of $C_i(t) - C_o(t)$ from experimental data

During drug efflux, the cellular DNR fluorescence intensity follows the dashed line and the cellular DNR fluorescence intensity *plus* medium DNR fluorescence intensity is represented by the experimentally obtained solid line in Scheme 1. The upper theoretical level, F_l (counts per s, cps), would be obtained if all the DNR were free in the extracellular solution after efflux. F_l (cps) exceeds the fluorescence intensity obtained after permeabilization of the plasma membrane by digitonin and equilibration of DNR across the plasma membrane, F_{eq} (cps), since some of the DNR will remain intercalated in DNA and its fluorescence intensity will be quenched. We define the cellular quenching factor, $q_{\pm Vp}$, as

$$q_{\pm Vp} = \frac{F_{\pm Vp}(t=0)}{F_l} \quad \text{(A3)}$$

in which $F_{\pm Vp}(t=0)$ (cps) is the cellular DNR fluorescence intensity at the start point of efflux in the absence or presence of verapamil.

At time zero, all DNR resides inside the cells. The fraction of intracellular DNR at time t, $x(t)$, is defined as:

$$x(t) = \frac{Q_i(t)}{Q_i(t=0)} \quad \text{(A4)}$$

in which $Q_i(t)$ (mol) is the cellular DNR content at time t.

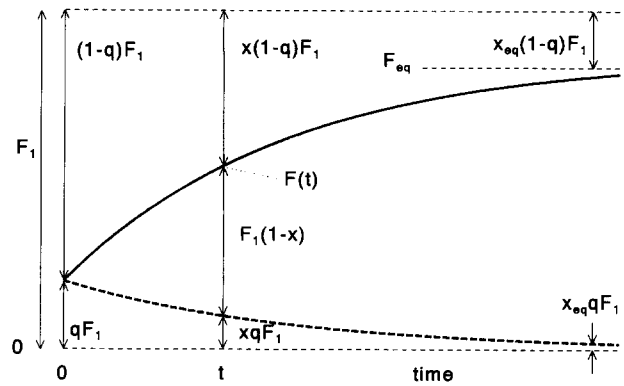

Scheme 1. Schematic representation of factors determining the daunorubicin (DNR) fluorescence intensity during efflux of cellular DNR. The fluorescence intensity of cellular DNR is represented by a dashed line and the (measured) total fluorescence intensity (of cells plus medium) by a solid line. At time t the total fluorescence, $F_{\pm Vp}(t)$, contains a contribution of the cellular DNR fluorescence intensity, $x(t)q_{\pm Vp}F_l$, and of the medium DNR fluorescence intensity, $(1-x(t))F_l$, and the signal would increase by $x(t)(1-q_{\pm Vp})F_l$ during complete efflux. F_{eq} refers to the fluorescence intensity obtained after plasma membrane permeabilization, $x(t)$ represents the fraction (relative to $t=0$) of intracellular DNR and $q_{\pm Vp}$ is the cellular quenching factor, due to DNA intercalation of DNR.

At $t=0$, $x(t)$ equals 1 and the fluorescence intensity of the intracellular DNR is quenched to $q_{\pm Vp}F_l$. At time t, the fluorescence intensity of the intracellular DNR equals $x(t)q_{\pm Vp}F_l$ and the fluorescence intensity of the extracellular fraction, $(1-x(t))$, equals $(1-x(t))F_l$.

The intracellular free drug concentration, $C_i(t)$, can be written as:

$$C_i(t) = \frac{\varepsilon F_l}{V_{cells}(C_i(t))}x(t) \quad \text{(A5)}$$

in which ε (mol cps^{-1}) is a constant that relates the medium DNR fluorescence to the amount of DNR in the medium, as can be determined by adding a known DNR concentration to the incubation mixture. $V_{cells}(C_i(t))$ (l) is the apparent distribution volume for DNR of the cells, defined as

$$V_{cells}(C_i(t)) = \frac{Q_i(t)}{C_i(t)} \quad \text{(A6)}$$

The extracellular free drug concentration, $C_o(t)$, can be written as:

$$C_o(t) = \frac{\varepsilon F_l}{V_{out}}(1-x(t)) \quad \text{(A7)}$$

in which V_{out} (l) represents the extracellular or efflux medium volume and is related to the apparent total volume, $V_{tot}(C_i(t))$ (l), by: $V_{tot}(C_i(t)) = V_{cells}(C_i(t)) + V_{out}$. Since the apparent distribution volume varies with the intracellular free drug concentration, the apparent total volume also depends on $C_i(t)$. Combination of Eqs. (A5) and (A7) yields an expression for the free drug concentra-

tion difference across the plasma membrane as a function of the fraction of intracellular DNR:

$$C_i(t) - C_o(t) = \frac{\varepsilon F_1}{V_{out}} \left(x(t) \frac{V_{tot}(C_i(t))}{V_{cells}(C_i(t))} - 1 \right) \quad \text{(A8)}$$

Experimentally, we can determine the difference between the measured DNR fluorescence intensity after t s of efflux, $F_{\pm Vp}(t)$ and F_{eq}, the DNR fluorescence intensity after plasma membrane permeabilization with digitonin, when $C_i(t) - C_o(t) = 0$. From Scheme 1 it follows that

$$\left.\begin{aligned} F_{eq} &= F_1 - x_{eq} F_1(-q_{\pm Vp}) \\ F_{\pm Vp}(t) &= F_1 - x(t) F_1(1 - q_{\pm Vp}) \end{aligned}\right\} \quad \text{(A9)}$$

in which x_{eq} is defined as the intracellular fraction when $C_i(t) - C_o(t) = 0$. Substitution of this condition in Eq. (A8) leads to

$$x_{eq} = \frac{V_{cells}(C_{i,eq})}{V_{tot}(C_{i,eq})} \quad \text{(A10)}$$

Combination of Eqs. (A9) and (A10) yields:

$$F_{eq} - F_{\pm Vp}(t) = F_1(1 - q_{\pm Vp}) \left(x(t) - \frac{V_{cells}(C_{i,eq})}{V_{tot}(C_{i,eq})} \right) \quad \text{(A11)}$$

in which $V_{cells}(C_{i,eq})/V_{tot}(C_{i,eq})$ represents the fraction of the total cuvette volume accessible to the intracellular DNR, comprising the extra virtual volume arising from DNA binding. Since at relatively low cell densities $V_{cells}(C_{i,eq})/V_{tot}(C_{i,eq}) \ll 1$, Eq. (A9) shows that the error introduced by using F_{eq} instead of F_1 will be small when compared to other (experimental) errors.

Eq. (A11) yields $x(t)$ in terms of $F_{eq} - F_{\pm Vp}(t)$ which can subsequently be substituted in Eq. (A8) to yield:

$$\begin{aligned} C_i(t) - C_o(t) &= \frac{F_{eq} - F_{\pm Vp}(t)}{1 - q_{\pm Vp}} \cdot \frac{\varepsilon V_{tot}(C_i(t))}{V_{out} V_{cells}(C_i(t))} \\ &+ \frac{\varepsilon F_1}{V_{out}} \left(\frac{V_{cells}(C_{i,eq})}{V_{cells}(C_i(t))} \cdot \frac{V_{tot}(C_i(t))}{V_{tot}(C_{i,eq})} - 1 \right) \end{aligned} \quad \text{(A12)}$$

If the apparent distribution volume were independent of the intracellular free drug concentration, $V_{cells}(C_{i,eq})/V_{cells}(C_i(t))$ and $V_{tot}(C_{i,eq})/V_{tot}(C_i(t))$ would both equal 1 and the second term in Eq. (A12) would vanish. Since neither $V_{cells}(C_i(t))$ nor $V_{tot}(C_i(t))$ are known explicitly, it is not possible to calculate $C_i(t) - C_o(t)$ explicitly. However, since the free drug concentration difference across the plasma membrane depends on the activity of the pump *only* through $F_{eq} - F_{\pm Vp}(t)$, it is possible to compare $C_i(t) - C_o(t)$ in the presence and absence of pumping: when we wish to compare drug efflux rates in the presence and the absence of pumping at the same $C_i(t) - C_o(t)$, we can compare them also at the same $F_{eq} - F_{\pm Vp}(t)$

A.3. Deriving leak and pump kinetics from drug efflux curves

According to the kinetic model defined in the first part of this appendix, the total DNR efflux rate, $J(C_i(t), C_o(t))$ (mol s^{-1} (10^6 cells^{-1})), can be expressed as

$$J(C_i(t), C_o(t)) = J_l(C_i(t), C_o(t)) + J_p(C_i(t), C_o(t)) \quad \text{(A13)}$$

in which $J_l(C_i(t),C_o(t))$ represents the leak rate and $J_p(C_i(t),C_o(t))$ the pump rate. The DNR efflux rate in the presence of verapamil, when P-gp mediated DNR efflux is completely inhibited, $J_{+Vp}(C_i(t),C_o(t))$, can be written as

$$J_{+Vp}(C_i(t), C_o(t)) = J_l(C_i(t), C_o(t)) \quad \text{(A14)}$$

As a consequence, the pump rate can be obtained by subtracting the efflux rate in the presence of verapamil and in the absence of verapamil, provided that the two efflux rates were measured at the same values of $C_i(t)$ and $C_o(t)$:

$$\begin{aligned} &J_p(C_i(t), C_o(t)) \\ &= J(C_i(t), C_o(t)) - J_l(C_i(t), C_o(t)) \\ &= J_{-Vp}(C_i(t), C_o(t)) - J_{+Vp}(C_i(t), C_o(t)) \end{aligned} \quad \text{(A15)}$$

When the cells at the same cell density are loaded with the same *amount* of drug and the extracellular concentrations are equal in both the plus- and minus-verapamil case it can be shown that the concentration difference across the plasma membrane is equal in both cases. Consequently, efflux rates at the same extracellular concentration or the same fluorescence intensity may be subtracted:

$$J_p(F_{-Vp}(t)) = J_{-Vp}(F_{-Vp}(t)) - J_{+Vp}(F_{+Vp}(t)) \quad \text{(A16)}$$

or within the assumption of loading with the same amount:

$$\begin{aligned} J_p(F_{eq} - F_{-Vp}(t)) &= J_{-Vp}(F_{eq} - F_{-Vp}(t)) \\ &- J_{+Vp}(F_{eq} - F_{+Vp}(t)) \end{aligned} \quad \text{(A17)}$$

Since the fluorescence intensity difference, $F_{eq} - F_{\pm Vp}(t)$, is related to $C_i(t) - C_o(t)$ (Eq. (A12)), a plot of $J_l(F_{eq} - F_{+Vp}(t))$ versus $F_{eq} - F_{+Vp}(t)$ should reveal the dependence of passive drug efflux on $C_i(t) - C_o(t)$. Similarly, a plot of $J_p(F_{eq} - F_{-Vp}(t))$ versus $F_{eq} - F_{-Vp}(t)$ should reveal the dependence of the pump rate on $C_i(t) - C_o(t)$.

The rate of change of the DNR fluorescence intensity is related to the transport rate, $J(C_i(t),C_o(t))$, through:

$$J_{\pm Vp}(C_i(t),C_o(t)) \equiv \frac{dQ_o(t)}{dt} = \frac{d}{dt}(\varepsilon F_1(1-x(t))) = \frac{\varepsilon}{1-q_{\pm Vp}}\frac{d}{dt}(F_{\pm Vp}(t)) \quad \text{(A18)}$$

Together with Eq. (A12), this relation allows us to calculate how the transport rate (both in the absence and presence of verapamil) varies with the free drug concentration difference across the plasma membrane.

A.4. Calculation of the intracellular free drug concentration $C_i(t)$

The intracellular free drug concentration is determined from the total cellular DNR content, $Q_i(t)$. From Eq. (A5), $Q_i(t)$ can be written as:

$$Q_i(t) = \varepsilon F_1 x(t) = \varepsilon F_1\left(\frac{F_{eq}-F_{+Vp}(t)}{F_1(1-q_{+Vp})} + \frac{V_{cells}(C_{i,eq})}{V_{tot}(C_{i,eq})}\right) \approx \varepsilon\frac{F_{eq}-F_{+Vp}(t)}{1-q_{+Vp}} \quad \text{(A19)}$$

if $V_{cells}(C_{i,eq})/V_{tot}(C_{i,eq})$ is assumed to be much smaller than unity. The intracellular free drug concentration is determined with the experimentally determined relation between total cellular drug content and intracellular free drug concentration: the apparent distribution volume (unpublished results):

$$C_i(t) = \frac{Q_i(t)}{V_{cells}(C_i(t))} \quad \text{(A20)}$$

References

[1] Bradley, G., Juranka, P.F. and Ling, V. (1988) Biochim. Biophys. Acta 948, 87–128.

[2] Gottesman, M.M. and Pastan, I. (1993) Annu. Rev. Biochem. 62, 385–427.

[3] Juranka, P.F., Zastawny, R.L. and Ling, V. (1989) FASEB J. 3, 2583–2592.

[4] Borst, P. (1991) Rev. Oncol. 4, 87–105.

[5] Carlsen, S.A., Till, J.E. and Ling, V. (1977) Biochim. Biophys. Acta 467, 238–250.

[6] Lankelma, J., Spoelstra, E.C., Dekker, H. and Broxterman, H.J. (1990) Biochim. Biophys. Acta 1055, 217–222.

[7] Skovsgaard, T. (1977) Biochem. Pharm. 26, 215–222.

[8] Spoelstra, E.C., Westerhoff, H.V. and Lankelma, J. (1992) Eur. J. Biochem. 207, 567–579.

[9] Sehested, M., Skovsgaard, T., Van Deurs, B. and Winther-Nielsen, H. (1987) JNCI 78, 171–177.

[10] Peterson, C., Baurain, R. and Trouet, A. (1980) Biochem. Pharm. 29, 1687–1692.

[11] Hindenburg, A.A., Gervasoni, J.E., Krishna, S., Steward, V.J., Rosado, M., Lutzky, J., Bhalla, K., Baker, M.A. and Taub, R.N. (1989) Cancer Res. 49, 4607–4614.

[12] Schuurhuis, G.J., Broxterman, H.J., Lange, J.H.M.D., Pinedo, H.M., Van Heijningen, T.H.M., Kuiper, C.M., Scheffer, G.L., Scheper, R.J., Van Kalken, C.K., Baak, J.P.A. and Lankelma, J. (1991) Br. J. Cancer 64, 857–861.

[13] Chaires, J.B., Dattagupta, N. and Crothers, D.M. (1982) Biochemistry 21, 3933–3940.

[14] Tsuruo, T., Iida, H., Tsukagoshi, S. and Sakurai, Y. (1982) Cancer Res. 42, 4730–4733.

[15] Demant, E.J.F., Sehested, M. and Jensen, P.B. (1990) Biochim. Biophys. Acta 1055, 117–125.

[16] Horio, M., Pastan, I., Gottesman, M.M. and Handler, J.S. (1990) Biochim. Biophys. Acta 1027, 116–122.

[17] Tamai, I. and Safa, A.R. (1991) J. Biol. Chem. 266, 16796–16800.

[18] Guiral, M., Viratelle, O., Westerhoff, H.V. and Lankelma, J. (1994) FEBS Lett. 346, 141–145.

[19] Shen, D.W., Fojo, A., Chin, J.E., Roninson, I.B., Richert, N., Pastan, I. and Gottesman, M.M. (1986) Science 232, 643–645.

[20] Versantvoort, C.H.M., Broxterman, H.J., Feller, N., Dekker, H., Kuiper, C.M. and Lankelma, J. (1992) Int. J. Cancer 50, 906–911.

[21] Tarasiuk, J., Frezard, F., Garnier-Suillerot, A. and Gattegno, L. (1989) Biochim. Biophys. Acta 1013, 109–117.

[22] Lankelma, J., Mülder, H.S., Van Mourik, F., Wong Fong Sang, H.W., Kraayenhof, R. and Van Grondelle, R. (1991) Biochim. Biophys. Acta 1093, 147–152.

[23] Mülder, H.S., Van Grondelle, R., Westerhoff, H.V. and Lankelma, J. (1993) Eur. J. Biochem. 218, 871–882.

[24] Raviv, Y., Polard, H.B., Bruggemann, E.P., Pastan, I. and Gottesman, M.M. (1990) J. Biol. Chem. 265, 3975–3980.

[25] Speth, P.A.J., Linssen, P.C.M., Boezeman, J.B.M., Wessels, H.M.C. and Haanen, C. (1987) Cancer Chemother. Pharmacol. 20, 311–315.